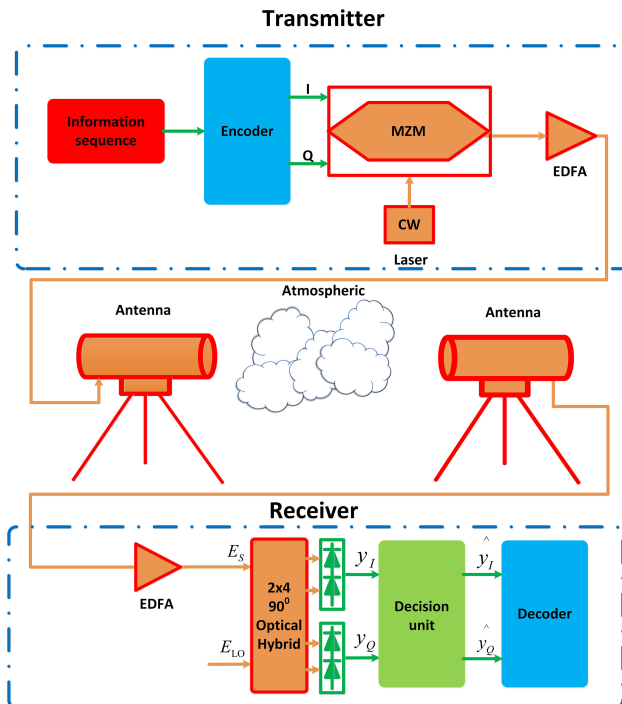


# Free-Space Optical Communication Using Coherent Detection and Double Adaptive Detection Thresholds

Volume 11, Number 1, February 2019

Lin Li  
Tianwen Geng  
Ye Wang  
Xueliang Li  
Jiabin Wu  
Yatian Li  
Shuang Ma  
Shijie Gao  
Zhiyong Wu



DOI: 10.1109/JPHOT.2018.2885542

1943-0655 © 2018 IEEE

# Free-Space Optical Communication Using Coherent Detection and Double Adaptive Detection Thresholds

Lin Li <sup>1,2</sup>, Tianwen Geng,<sup>1</sup> Ye Wang,<sup>1,2</sup> Xueliang Li,<sup>1,2</sup> Jiabin Wu,<sup>1</sup>  
Yatian Li,<sup>1,2</sup> Shuang Ma,<sup>1</sup> Shijie Gao,<sup>1</sup> and Zhiyong Wu<sup>1</sup>

<sup>1</sup>Changchun Institute of Optics, Fine Mechanics and Physics, Chinese Academy of Sciences, Changchun 130033, China

<sup>2</sup>University of Chinese Academy of Sciences, Beijing 100049, China

DOI:10.1109/JPHOT.2018.2885542

1943-0655 © 2018 IEEE. Translations and content mining are permitted for academic research only.

Personal use is also permitted, but republication/redistribution requires IEEE permission.

See [http://www.ieee.org/publications\\_standards/publications/rights/index.html](http://www.ieee.org/publications_standards/publications/rights/index.html) for more information.

Manuscript received October 21, 2018; accepted December 4, 2018. Date of publication December 7, 2018; date of current version December 28, 2018. This work was supported in part by the National Natural Science Foundation of China under Grant 51605465 and in part by the Research Project Of Scientific Research Equipment of Chinese Academy of Sciences. Corresponding author: Lin Li (e-mail: lili920329@126.com).

**Abstract:** In this paper, ON-OFF Keying free-space optical (FSO) communication with coherent detection and double adaptive detection thresholds is proposed. The 3-bit encoding and double adaptive detection thresholds presented in the scheme can significantly improve the system performance, and there is no need of acquiring the instantaneous channel state information and probability density function (pdf) of the turbulence model. In order to enhance the accuracy of the threshold even further, the decision-aided method is offered to set the second detection threshold. The pdfs of the detection thresholds and the average bit error rate (BER) of the system are theoretically derived. Numerical studies show that the performance of the system is comparable to the performance of the idealized adaptive detection system and the loss of the signal-to-noise ratio (SNR) performance is only 1 dB at a BER of  $10^{-9}$  over a lognormal turbulence channel with normalized standard deviation of irradiance  $\sigma = 0.25$  and phase noise with normalized variance  $\sigma_\phi^2 = 0.07$ . Hence, this scheme can contribute to the performance improvement of the FSO system and its practical realization.

**Index Terms:** Coherent communication, free space communication.

## 1. Introduction

Free-Space optical communication has been a good candidate for next generation broadband services since it supports large bandwidth, quick and inexpensive setup, unlicensed spectrum, and excellent security [1]. However, the performance of FSO systems can be degraded by atmospheric turbulence [2]. In order to mitigate the influence of atmospheric turbulence, various methods, including channel diversity, symbol interleaving, and adaptive detection threshold have been given. Among those methods, adaptive detection threshold has received considerable interest recently [3]–[5], since it allows systems to achieve better average BER with low complexity.

While, how to set the adaptive detection threshold remains to be a problem. Previous research tends to assume detection with instantaneous channel state information [6]–[10]. Alternatively, research has also suggested that the fading intensity must be estimated with the help of redundant overhead, such as training sequences or pilot symbols [11]. In [12], the authors introduced

pilot-symbol assisted modulation and maximum likelihood method which could mitigate the effects of turbulence and improve the system performance. However, it required the temporal joint and marginal PDF of the channel. In practice, for ease of commercial implementation and to facilitate infrastructure transparency, detection without CSI and PDF of the turbulence channel is the preferred methodology [13].

In [14], the authors analyzed the performance improvement of on–off-keying free-space optical communication systems in atmospheric turbulence conditions due to coherent detection and the dynamic decision threshold (DDT) scheme. The results showed that the DDT scheme provided a 5.7 dB power reduction for achieving a bit error rate of  $10^{-3}$  compared with the conventional fixed decision threshold scheme.

In [15], the authors have done a pioneering work, which a source information transformation system has been proposed. Multiple optical wavelengths are used to get the adaptive detection thresholds in this system. It's shown that such system can achieve an acceptable BER performance without requiring the knowledge of the instantaneous CSI and the PDF of the turbulence model.

In this study, to achieve better thresholds and system performance, an OOK free-space optical communication system with CD-DADT is designed. At the transmitter, 3-bit encoding is utilized to transmit the information. At the receiver, two adaptive thresholds are designed to detect the inphase and quadrature branches of signal without the instantaneous CSI and the PDF of the channel model. To improve the precision of the threshold even further, we also offer the decision–aided method to set the second detection threshold. Numerical studies show that such a system provides good BER performance which is comparable to the performance of the idealized adaptive detection system.

The remainder of the paper is organized as follows. In Section 2, the system structure and model are introduced. The PDFs of the detection thresholds are obtained in Section 3. Section 4 derives the average BER of the system. Numerical results and discussions are provided in Section 5. Finally, some concluding remarks are provided in Section 6.

## 2. System Structure and Model

### 2.1 System With Double Rapid Detection Thresholds

We consider an intensity modulation and coherent detection system over atmospheric turbulence channel. The synchronism of the local oscillator in the receiver and the bit and frame synchronization for the coding and decoding process are assumed to be ideal. We also assume that samples from the transmitted rectangular analog pulses are perfect. The scheme and model of the system are as follows.

The structure of the system is described in Fig. 1. At the transmitter, a Mach–Zehnder modulator (MZM) is used to modulate the beam. The in-phase and the quadrature branches of the MZM are used to transmit special coded information which can ensure that at least one branch transmits bit “1” during each symbol duration. The encoder is designed to get the special coded information. As shown in Fig. 2, first, a 3-bit binary information sequence  $a_3a_2a_1$  is converted to a ternary information sequence  $b_2b_1$ . Then each ternary symbol  $\{0, 1, 2\}$  in the sequence is mapped into a 2-bit binary sequence  $\{01, 10, 11\}$  which the all-zero sequence is not contained. Finally, after the serial-to-parallel conversion, the two bits of the resulting binary sequence are sent to the two branches of the MZM respectively. The signal sent by the transmitter can be written as

$$S(t) = E_I [A(t) \cos(2\pi f_c t) + B(t) \sin(2\pi f_c t)], \quad (1)$$

where  $E_I$  is the amplitude of transmitting,  $A(t)$  and  $B(t) \in \{0, 1\}$  are the data in the two branches,  $f_c$  is the frequency of the carrier wave.

At the receiver, a homodyne inphase-quadrature receiver (IQ-receiver) is used for signal detection. The received signal beats with the local oscillator (LO) in a  $90^\circ$  optical hybrid, and the output signals are detected by two balanced photodetectors.

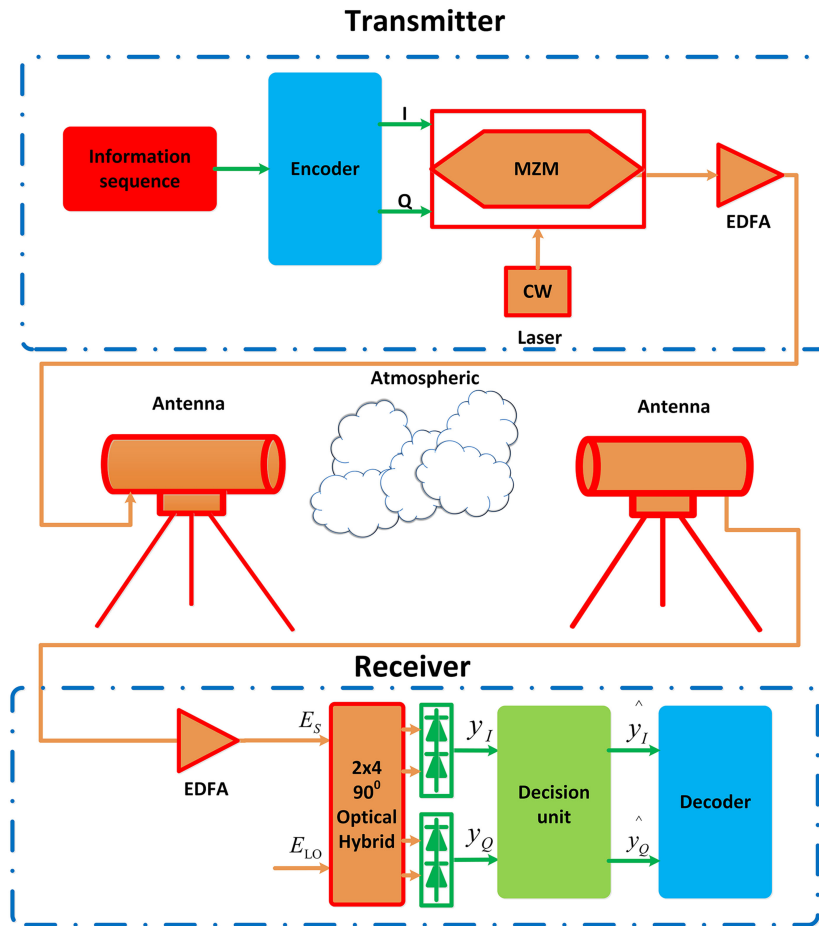


Fig. 1. The structure of the system. MZM: Mach-Zehnder Modulator, CW: Continuous Wave Laser, EDFA: Erbium-Doped Fiber Amplifier.

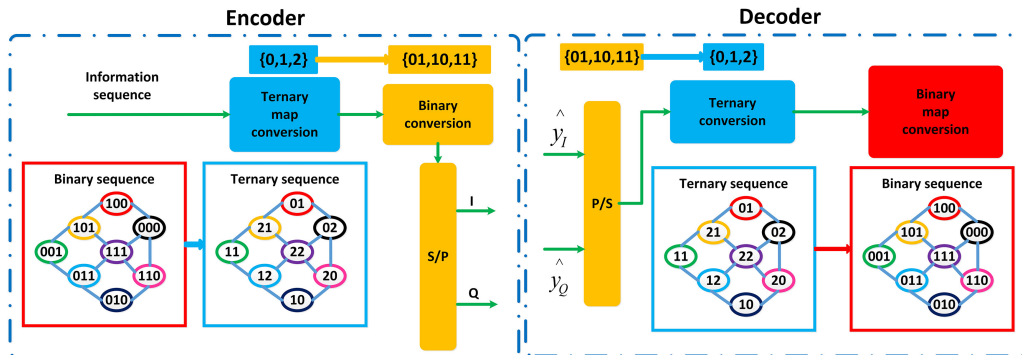


Fig. 2. The structure of the encoder and decoder. S/P: Serial-to-Parallel Conversion, P/S: Parallel-to-Serial Conversion.

The received signals are affected by the great attenuation of the atmospheric channel. Normally, the attenuation can be regarded as constant and can be compensated by the erbium-doped fiber amplifier in the receiver.

The two branches of the received signals also suffer from atmospheric turbulence induced fading which can be expressed as a multiplicative stationary random process  $h(t)$ . The channel fading  $h(t)$

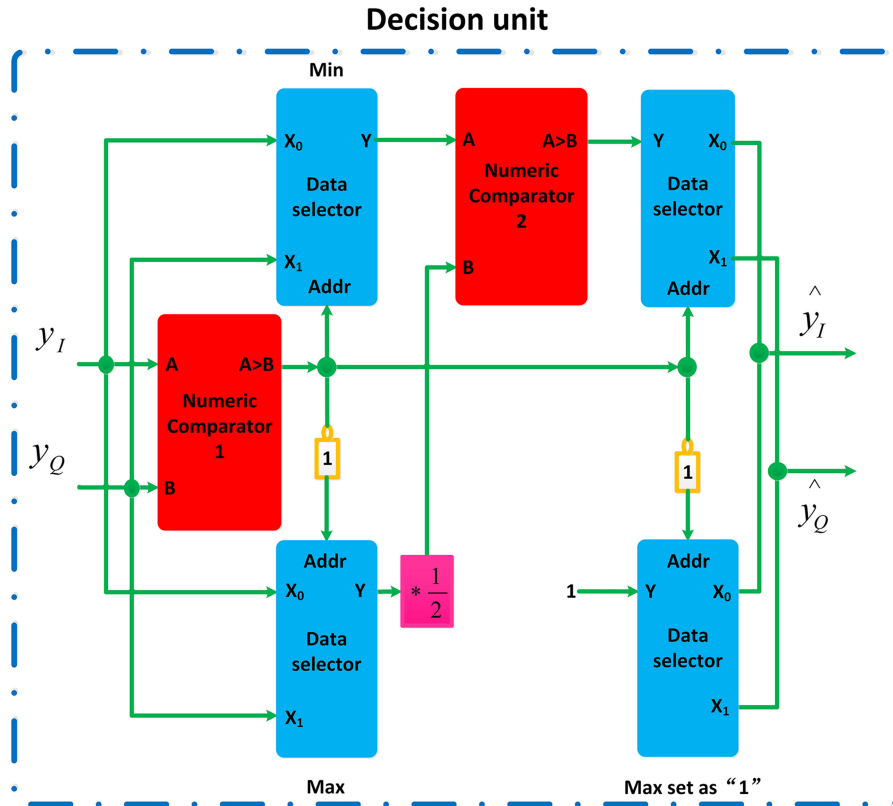


Fig. 3. The structure of the decision unit.

is assumed to be same for the two branches of the signals at the same time [16]. The received signals also suffer from the phase fluctuations that the turbulence induced. The phase fluctuations obey zero-mean Gaussian statistics with variance  $\sigma_\phi^2$  [17].

So at the receiver, after the balanced photodetectors the signals can be written as

$$\begin{aligned} y_I(t) &= RE_I E_{LO} h(t) [A(t) \cos(\varphi_n) + B(t) \sin(\varphi_n)] + n_1(t) \\ y_Q(t) &= RE_I E_{LO} h(t) [B(t) \cos(\varphi_n) + A(t) \sin(\varphi_n)] + n_2(t), \end{aligned} \quad (2)$$

where  $E_{LO}$  is the amplitude of the local oscillator,  $\varphi_n$  is the phase noise caused by atmospheric turbulence,  $R$  is the photodetector responsivity,  $n_1(t)$  and  $n_2(t)$  are additive white Gaussian noise due to thermal noise and shot noise in receiver with total power  $\sigma_g^2$  [18]. For convenience, we set  $R$  as 1 in the rest of the paper.

After the two balanced photodetectors are the decision unit and the decoder. As shown in Fig. 3, the decision unit is composed of some simple devices, such as the numeric comparator, data selector, multiplexer, and NOT gate. The structure of the decoder is given in Fig. 2.

For an intensity modulation and direct detection (IM/DD) system with instantaneous CSI, the optimal maximum-likelihood-based decision thresholds can be expressed by [12]

$$T_{th} = \frac{\sigma_0 h_1 + \sigma_1 h_0}{\sigma_0 + \sigma_1}, \quad (3)$$

where  $h_1$  and  $h_0$  are averages of the generated currents at the receiver for symbols "1" and "0",  $\sigma_1$  and  $\sigma_0$  are the standard deviations of the noise currents for symbols "1" and "0". For simplicity, we set  $\sigma_0 = \sigma_1 = \sigma_g$ ,  $h_0 = 0$  and  $h_1 = h$ . Then the optimal detection thresholds can be written as  $T_{th} = h/2$ .

In practice, this approach is difficult to realize, owing to the fact that the instantaneous CSI is required to detect the signals. However, for our system, when average SNR (denoted by  $\gamma$ ) is large enough and the phase noise is small enough, we can assume that

$$\lim_{\gamma \rightarrow \infty, \varphi_n \rightarrow 0} \max \{y_I, y_Q\} = h. \quad (4)$$

Thus, the double detection thresholds at the decision unit can be intuitively set as

$$\begin{aligned} T_{th1} &= \min \{y_I, y_Q\} \\ T_{th2} &= \frac{1}{2} \max \{y_I, y_Q\}, \end{aligned} \quad (5)$$

where  $T_{th1}$  is the threshold for the larger branch at numeric comparator 1 of the decision unit and  $T_{th2}$  is the threshold for the smaller branch at numeric comparator 2 of the decision unit. Here, we define this kind of thresholds as rapid detection thresholds and the rest of this paper follows this definition.

So in each symbol duration, the receiver sets the larger signal as “1” and the value of one-half of the larger received signal as the detection thresholds for the other received signal. This can prevent the situation that all of the signals on the two branches are detected as bit “0”. Then the output signals  $\hat{y}_I$  and  $\hat{y}_Q$  of decision unit can be written as

$$\begin{aligned} \hat{y}_I &= \max \left\{ S[y_I - \min(y_I, y_Q)], S\left[y_I - \frac{1}{2} \max(y_I, y_Q)\right] \right\} \\ \hat{y}_Q &= \max \left\{ S[y_Q - \min(y_I, y_Q)], S\left[y_Q - \frac{1}{2} \max(y_I, y_Q)\right] \right\}, \end{aligned} \quad (6)$$

where

$$S(x) = \begin{cases} 0, & x \leq 0 \\ 1, & x > 0 \end{cases}. \quad (7)$$

After that every two groups of the parallel output signals will be sent to the decoder and then converted to a ternary sequence  $\hat{b}_2\hat{b}_1$ . Finally, the ternary sequence will be mapped back to the binary information sequence  $\hat{a}_3\hat{a}_2\hat{a}_1$  as shown in Fig. 2.

In this way, the system can achieve rapid detection thresholds adjustments without requiring instantaneous CSI and complex devices like the analog-to-digital (AD) circuits.

## 2.2 System With Decision–Aided Thresholds

Although the system with double rapid detection thresholds is easy to achieve, it may also cause potentially significant degradation in error performance. This is due to the fact that the detection threshold for the smaller received signal is decided by one-half of the larger received signal in each symbol duration. This detection threshold is optimum only when the electrical SNR approaches infinity and the phase fluctuations approaches 0. When the SNR is not high enough and the phase fluctuations are strong, the detection threshold will not be an optimum detection threshold for the system.

For a practical lasercom system, the data symbol durations (500 ps for example) would exceed the atmospheric time constant (which is of the order of 1 ms) by many orders of magnitude. The atmospheric turbulence can be seen as constant over a frame with a suitable length ( $10^6$  bit for example).

In order to improve the precision of the threshold, the decision–aided threshold estimation is offered to set the second detection threshold.

We consider a frame of  $N$  bit intervals. First, we set the thresholds  $T_{th1}'$  and  $T_{th2}'$  of the system as

$$\begin{aligned} T_{th1}' &= \min \{y_I(k), y_Q(k)\} \\ T_{th2}' &= \frac{1}{2N} \sum_{k=1}^N \max \{y_I(k), y_Q(k)\}. \end{aligned} \quad (8)$$

When  $N$  is large enough, we have

$$T_{th2}' = \frac{\overline{h \cos(\varphi_n)}}{2} + n_{w1}, \quad (9)$$

where  $\overline{\cos(\varphi_n)}$  is the average of  $\cos(\varphi_n)$  during the frame and  $n_{w1}$  is an additive white Gaussian noise with variance  $\sigma_g^2/2N$ . Then, after comparing with the thresholds, the output signals  $\hat{y}_I$  and  $\hat{y}_Q$  of two branches can be written as

$$\begin{aligned} \hat{y}_I &= \max \left\{ S[y_I - \min(y_I, y_Q)], S \left[ y_I - \frac{1}{2N} \sum_{k=1}^N \max \{y_I(k), y_Q(k)\} \right] \right\} \\ \hat{y}_Q &= \max \left\{ S[y_Q - \min(y_I, y_Q)], S \left[ y_Q - \frac{1}{2N} \sum_{k=1}^N \max \{y_I(k), y_Q(k)\} \right] \right\}. \end{aligned} \quad (10)$$

Under the assumption that the decisions made via Eq. (10) are accurate we employ the results of the first decision to get decision-aided detection thresholds as

$$T_{th2}'' = \frac{1}{2} \left( \frac{1}{N} \sum_{k=1}^N \max \{y_I(k), y_Q(k)\} + \frac{1}{M} \sum_{k=1}^M r_0(k) \right), \quad (11)$$

where

$$\begin{aligned} M &= \sum_{k=1}^N S(T_{th2}' - \min \{y_I(k), y_Q(k)\}) \\ r_0(k) &= S(T_{th2}' - \min \{y_I(k), y_Q(k)\}) \cdot \min \{y_I(k), y_Q(k)\}. \end{aligned} \quad (12)$$

Then we have

$$T_{th2}'' = \frac{\overline{h \cos(\varphi_n)} + \overline{h \sin(\varphi_n)}}{2} + n_{w1} + n_{w2}, \quad (13)$$

where  $\overline{\sin(\varphi_n)}$  is the average of  $\sin(\varphi_n)$  during the frame and  $n_{w2}$  is an additive white Gaussian noise sample with variance equal to  $\sigma_g^2/2M$ . The quality of the thresholds improves with increasing  $N$ .

After comparing with the thresholds, the final output signals  $\hat{y}'_I$ ,  $\hat{y}'_Q$  of two branches can be written as

$$\begin{aligned} \hat{y}'_I &= \max \left\{ S[y_I - \min(y_I, y_Q)], S \left[ y_I - \frac{1}{2} \left( \frac{1}{N} \sum_{k=1}^N \max \{y_I(k), y_Q(k)\} + \frac{1}{M} \sum_{k=1}^M r_0(k) \right) \right] \right\} \\ \hat{y}'_Q &= \max \left\{ S[y_Q - \min(y_I, y_Q)], S \left[ y_Q - \frac{1}{2} \left( \frac{1}{N} \sum_{k=1}^N \max \{y_I(k), y_Q(k)\} + \frac{1}{M} \sum_{k=1}^M r_0(k) \right) \right] \right\}. \end{aligned} \quad (14)$$

Finally, the output signals will be decoded by the decoder in Fig. 2 as mentioned before.

### 3. PDFs of the Double Rapid Detection Thresholds

The PDFs of the rapid detection thresholds  $T_{th1}$ ,  $T_{th2}$  are obtained in this section. First, a lognormally distributed fading channel is considered. The lognormal distribution is given by

$$f(h) = \frac{1}{\sqrt{8\pi}h\sigma} \exp\left(-\frac{[\ln(h) + 2\sigma^2]^2}{8\sigma^2}\right), \quad (15)$$

where  $\sigma^2$  is the log-amplitude variance and  $h \geq 0$ . We also assume that the LO amplitude  $E_{LO}$  and transmitting amplitude  $E_I$  are unity. Then we derive the conditional PDFs of  $T_{th1}$  and  $T_{th2}$ .

The conditional pdfs of  $T_{th1}$ ,  $T_{th2}$  vary with the different ternary symbols that the transmitter sends. When the transmitter sends "0", the two branches of signals can be expressed as

$$\begin{aligned} y_{I0}(t) &= h \sin(\varphi_n) + n_1 \\ y_{Q0}(t) &= h \cos(\varphi_n) + n_2. \end{aligned} \quad (16)$$

When the transmitter sends "1", the signals can be obtained as

$$\begin{aligned} y_{I1}(t) &= h \cos(\varphi_n) + n_1 \\ y_{Q1}(t) &= h \sin(\varphi_n) + n_2. \end{aligned} \quad (17)$$

Then the conditional cumulative distribution functions of  $T_{th1}$ ,  $T_{th2}$  can be written as

$$\begin{aligned} F_{T_{th1}}(t_{th1} | h, \varphi_n, 0) &= F_{T_{th1}}(t_{th1} | h, \varphi_n, 1) \\ &= P(\min\{h \sin(\varphi_n) + n_1, h \cos(\varphi_n) + n_2\} < t_{th1}) \\ &= P(n_1 < t_{th1} - h \sin(\varphi_n) \cup n_2 < t_{th1} - h \cos(\varphi_n)) \\ F_{T_{th2}}(t_{th2} | h, \varphi_n, 0) &= F_{T_{th2}}(t_{th2} | h, \varphi_n, 1) \\ &= P\left(\frac{\max\{h \sin(\varphi_n) + n_1, h \cos(\varphi_n) + n_2\}}{2} < t_{th2}\right) \\ &= P(n_1 < 2t_{th2} - h \sin(\varphi_n), n_2 < 2t_{th2} - h \cos(\varphi_n)). \end{aligned} \quad (18)$$

Since all the noise components  $n_1(t)$ ,  $n_2(t)$  are assumed to be independent and identically distributed, we have

$$\begin{aligned} &P(n_1 < t_{th1} - h \sin(\varphi_n) \cup n_2 < t_{th1} - h \cos(\varphi_n)) \\ &= P(n_1 < t_{th1} - h \sin(\varphi_n)) + P(n_2 < t_{th1} - h \cos(\varphi_n)) \\ &\quad - P(n_1 < t_{th1} - h \sin(\varphi_n)) P(n_2 < t_{th1} - h \cos(\varphi_n)) \\ &P(n_1 < 2t_{th} - h \sin(\varphi_n), n_2 < 2t_{th} - h \cos(\varphi_n)) \\ &= P(n_1 < 2t_{th} - h \sin(\varphi_n)) P(n_2 < 2t_{th} - h \cos(\varphi_n)). \end{aligned} \quad (19)$$

It follows that

$$\begin{aligned} F_{T_{th1}}(t_{th1} | h, \varphi_n, 0) &= F_{T_{th1}}(t_{th1} | h, \varphi_n, 1) \\ &= \Phi\left[\frac{t_{th1} - h \sin(\varphi_n)}{\sigma_g}\right] + \Phi\left[\frac{t_{th1} - h \cos(\varphi_n)}{\sigma_g}\right] \\ &\quad - \Phi\left[\frac{t_{th1} - h \sin(\varphi_n)}{\sigma_g}\right] \Phi\left[\frac{t_{th1} - h \cos(\varphi_n)}{\sigma_g}\right] \\ F_{T_{th2}}(t_{th2} | h, \varphi_n, 0) &= F_{T_{th2}}(t_{th2} | h, \varphi_n, 1) \\ &= \Phi\left[\frac{2t_{th2} - h \sin(\varphi_n)}{\sigma_g}\right] \Phi\left[\frac{2t_{th2} - h \cos(\varphi_n)}{\sigma_g}\right]. \end{aligned} \quad (20)$$

So the conditional pdfs can be written as

$$\begin{aligned}
 f_{T_{th1}}(t_{th1} | h, \varphi_n, 0) &= f_{T_{th1}}(t_{th1} | h, \varphi_n, 1) \\
 &= f_N [t_{th1} - h \sin(\varphi_n)] + f_N [t_{th1} - h \cos(\varphi_n)] \\
 &\quad - \phi \left[ \frac{t_{th1} - h \sin(\varphi_n)}{\sigma_g} \right] f_N [t_{th1} - h \cos(\varphi_n)] \\
 &\quad - \phi \left[ \frac{t_{th1} - h \cos(\varphi_n)}{\sigma_g} \right] f_N [t_{th1} - h \sin(\varphi_n)] \\
 f_{T_{th2}}(t_{th2} | h, \varphi_n, 0) &= f_{T_{th2}}(t_{th2} | h, \varphi_n, 1) \\
 &= \phi \left[ \frac{2t_{th2} - h \sin(\varphi_n)}{\sigma_g} \right] f_N [2t_{th2} - h \cos(\varphi_n)] \\
 &\quad + \phi \left[ \frac{2t_{th2} - h \cos(\varphi_n)}{\sigma_g} \right] f_N [2t_{th2} - h \sin(\varphi_n)]. \tag{21}
 \end{aligned}$$

When the transmitter sends “2”, the two branches of signals can be expressed as

$$\begin{aligned}
 y_{I2}(t) &= \sqrt{2}h \cos\left(\varphi_n - \frac{\pi}{4}\right) + n_1 \\
 y_{Q2}(t) &= \sqrt{2}h \cos\left(\varphi_n - \frac{\pi}{4}\right) + n_2. \tag{22}
 \end{aligned}$$

Then the conditional cumulative distribution functions of  $T_{th1}$ ,  $T_{th2}$  can be written as

$$\begin{aligned}
 F_{T_{th1}}(t_{th1} | h, \varphi_n, 2) &= P\left(\min\left\{\sqrt{2}h \cos\left(\varphi_n - \frac{\pi}{4}\right) + n_1, \sqrt{2}h \cos\left(\varphi_n - \frac{\pi}{4}\right) + n_2\right\} < t_{th1}\right) \\
 &= 2\phi \left[ \frac{1}{\sigma_g} \left[ t_{th1} - \sqrt{2}h \cos\left(\varphi_n - \frac{\pi}{4}\right) \right] \right] - \phi^2 \left[ \frac{1}{\sigma_g} \left[ t_{th1} - \sqrt{2}h \cos\left(\varphi_n - \frac{\pi}{4}\right) \right] \right] \\
 F_{T_{th2}}(t_{th2} | h, \varphi_n, 2) &= P\left(\frac{1}{2} \max\left\{\sqrt{2}h \cos\left(\varphi_n - \frac{\pi}{4}\right) + n_1, \sqrt{2}h \cos\left(\varphi_n - \frac{\pi}{4}\right) + n_2\right\} < t_{th2}\right) \\
 &= \phi^2 \left[ \frac{1}{\sigma_g} \left[ 2t_{th2} - \sqrt{2}h \cos\left(\varphi_n - \frac{\pi}{4}\right) \right] \right], \tag{23}
 \end{aligned}$$

and the conditional PDFs can be obtained as

$$\begin{aligned}
 f_{T_{th1}}(t_{th1} | h, \varphi_n, 2) &= 2f_N \left[ t_{th1} - \sqrt{2}h \cos\left(\varphi_n - \frac{\pi}{4}\right) \right] - 2\phi \left[ \frac{1}{\sigma_g} \left[ t_{th1} - \sqrt{2}h \cos\left(\varphi_n - \frac{\pi}{4}\right) \right] \right] f_N \left[ t_{th1} - \sqrt{2}h \cos\left(\varphi_n - \frac{\pi}{4}\right) \right] \\
 f_{T_{th2}}(t_{th2} | h, \varphi_n, 2) &= 2\phi \left[ \frac{1}{\sigma_g} \left[ 2t_{th2} - \sqrt{2}h \cos\left(\varphi_n - \frac{\pi}{4}\right) \right] \right] f_N \left[ 2t_{th2} - \sqrt{2}h \cos\left(\varphi_n - \frac{\pi}{4}\right) \right], \tag{24}
 \end{aligned}$$

where  $\phi(x) = \int_{-\infty}^x \frac{1}{\sqrt{2\pi}} \exp(-\frac{r^2}{2}) dr$  and  $f_N(x) = \frac{1}{\sqrt{2\pi\sigma_g^2}} \exp(-\frac{x^2}{2\sigma_g^2})$ . Then the conditional PDFs of  $T_{th1}$ ,  $T_{th2}$  on  $h$  and  $\varphi_n$  can be expressed as

$$\begin{aligned} f_{T_{th1}}(t_{th1} | h, \varphi_n) &= \sum_{k=0}^2 f_{T_{th1}}(t_{th1} | h, \varphi_n, k) p(k) \\ f_{T_{th2}}(t_{th2} | h, \varphi_n) &= \sum_{k=0}^2 f_{T_{th2}}(t_{th2} | h, \varphi_n, k) p(k), \end{aligned} \quad (25)$$

where  $p(k)$  is the probability that symbol “ $k$ ” is transmitted and  $p(0) = 1/4$ ,  $p(1) = p(2) = 3/8$ . Averaging the conditional PDFs with respect to  $h$  and  $\varphi_n$ , finally, we have the PDFs of  $T_{th1}$ ,  $T_{th2}$  as

$$\begin{aligned} f_{T_{th1}}(t_{th1}) &= E_h [E_{\varphi_n} [f_{T_{th1}}(t_{th1} | h, \varphi_n)]] \\ f_{T_{th2}}(t_{th2}) &= E_h [E_{\varphi_n} [f_{T_{th2}}(t_{th2} | h, \varphi_n)]], \end{aligned} \quad (26)$$

where  $E_h[\cdot]$  and  $E_{\varphi_n}[\cdot]$  represent the statistical expectation with respect to  $h$  and  $\varphi_n$ . The PDFs of the double adaptive detection thresholds given by Eq. (26) can be useful in FSO system design.

#### 4. The Average BER of the System With Double Rapid Detection Thresholds

In this section, the average BER of the system with rapid detection thresholds is derived under a lognormally distributed fading channel. To achieve this purpose, first we derive the conditional probability of the received ternary symbol. After that the average BER of the system is given.

##### 4.1 The Conditional Probability of the Received Ternary Symbol $\hat{b}_j$ Given the Transmitted Ternary Symbol $b_j$

The detection thresholds of the system vary with the different ternary symbols that the transmitter sends. When the transmitter sends “0”, the detection thresholds becomes

$$\begin{aligned} T_{th1}(0) &= \min \{h \sin(\varphi_n) + n_1, h \cos(\varphi_n) + n_2\} \\ T_{th2}(0) &= \frac{1}{2} \max \{h \sin(\varphi_n) + n_1, h \cos(\varphi_n) + n_2\}. \end{aligned} \quad (27)$$

When the transmitter sends “1”, the detection thresholds becomes

$$\begin{aligned} T_{th1}(1) &= \min \{h \cos(\varphi_n) + n_1, h \sin(\varphi_n) + n_2\} \\ T_{th2}(1) &= \frac{1}{2} \max \{h \cos(\varphi_n) + n_1, h \sin(\varphi_n) + n_2\}. \end{aligned} \quad (28)$$

When the transmitter sends “2”, the detection thresholds becomes

$$\begin{aligned} T_{th1}(2) &= \min \left\{ \sqrt{2}h \cos\left(\varphi_n - \frac{\pi}{4}\right) + n_1, \sqrt{2}h \cos\left(\varphi_n - \frac{\pi}{4}\right) + n_2 \right\} \\ T_{th2}(2) &= \frac{1}{2} \max \left\{ \sqrt{2}h \cos\left(\varphi_n - \frac{\pi}{4}\right) + n_1, \sqrt{2}h \cos\left(\varphi_n - \frac{\pi}{4}\right) + n_2 \right\}. \end{aligned} \quad (29)$$

Comparing the two branches of signals with the detection thresholds, the conditional probability of the received ternary symbol can be calculated. For the limitation of length, we only derive the conditional probability  $P(0|0)$  in this section. Other conditional probabilities of the system are given in the Appendix. The conditional probability  $P(0|0)$  can be written as

$$P(0|0) = E_h \left[ E_{\varphi_n} \left[ P \left( h \cos(\varphi_n) + n_2 > h \sin(\varphi_n) + n_1 \cap \frac{h \cos(\varphi_n) + n_2}{2} > h \sin(\varphi_n) + n_1 | h, \varphi_n \right) \right] \right]. \quad (30)$$

#### 4.2 Average BER of the System With Double Rapid Detection Thresholds

To calculate the average BER of the system, the conditional probabilities of the received ternary symbol  $\hat{b}_l$  given the transmitted ternary symbol  $b_l$  calculated in the front are used. Since the ternary symbols  $\hat{b}_l$  and  $b_l$  are independent when  $l$  is different, the conditional probability for  $\hat{b}_2\hat{b}_1$  given  $b_2b_1$  can be written as

$$P(\hat{b}_2\hat{b}_1 | b_2b_1) = \prod_{j=1}^2 P(\hat{b}_j | b_2b_1) = \prod_{j=1}^2 P(\hat{b}_j | b_j). \quad (31)$$

So the conditional probability of the received binary sequence  $\hat{a}_3\hat{a}_2\hat{a}_1$  given the transmitted binary sequence  $a_3a_2a_1$  can be expressed as

$$P(\hat{a}_3\hat{a}_2\hat{a}_1 | a_3a_2a_1) = P(\hat{b}_2\hat{b}_1 | b_2b_1) = \prod_{j=1}^2 P(\hat{b}_j | b_j). \quad (32)$$

Then we have

$$P(\hat{a}_3\hat{a}_2\hat{a}_1, a_3a_2a_1) = P(\hat{a}_3\hat{a}_2\hat{a}_1 | a_3a_2a_1) P(a_3a_2a_1), \quad (33)$$

where  $P(a_3a_2a_1) = 1/2^3$  is the probability that binary sequence  $a_3a_2a_1$  is transmitted.

The conditional error probability of the system given  $a_3a_2a_1$  and  $\hat{a}_3\hat{a}_2\hat{a}_1$  can be written as

$$P(e | \hat{a}_3\hat{a}_2\hat{a}_1, a_3a_2a_1) = \frac{\sum_{l=1}^3 a_l \oplus \hat{a}_l}{3}, \quad (34)$$

where  $\oplus$  implements an exclusive OR. So we have the average BER of the system as

$$\begin{aligned} P(e) &= \sum_{a_3a_2a_1, \hat{a}_3\hat{a}_2\hat{a}_1} P(e | \hat{a}_3\hat{a}_2\hat{a}_1, a_3a_2a_1) \times P(\hat{a}_3\hat{a}_2\hat{a}_1, a_3a_2a_1) \\ &= \frac{1}{2^3} \sum_{a_3a_2a_1, \hat{a}_3\hat{a}_2\hat{a}_1} \frac{\sum_{l=1}^3 a_l \oplus \hat{a}_l}{3} \prod_{j=1}^2 P(\hat{b}_j | b_j). \end{aligned} \quad (35)$$

## 5. Numerical Results

As we discussed in Section 2, the first detection threshold of the CD-DADT system is set as rapid detection threshold and the second detection threshold of the systems can be set as rapid detection threshold or decision-aided threshold. So in this section, the PDF of the detection thresholds given in Section 3 will be verified and the BER performance of the system with different second detection thresholds will be numerically studied.

First, a lognormally distributed fading channel is considered. The log-amplitude variance  $\sigma^2$  can be represented by Rytov variance  $\sigma_R^2$  for a plane wave in weak fluctuation theory as

$$\sigma^2 = \frac{\sigma_R^2}{4} = \frac{1}{4} (1.23 C_n^2 k^{7/6} L^{11/6}), \quad (36)$$

where  $C_n^2$  is the atmospheric structure constant,  $k = 2\pi/\lambda$  is the wave number and  $L$  is the propagation distance [19]. For a FSO system near the ground, the atmospheric structure constant varies from  $10^{-17} \text{ m}^{-2/3}$  to  $10^{-13} \text{ m}^{-2/3}$  according to the atmospheric turbulence conditions [17].

Then the phase noise  $\varphi_n$  is assumed to obey the zero-mean Gaussian statistics and its variance can be expressed as

$$\sigma_\phi^2 = C_J \left( \frac{D}{r_0} \right)^{5/3}, \quad (37)$$

TABLE 1  
Parameters Used in the Numerical Simulation

Parameter	Value I	Value II	Value III
Wavelength $\lambda$	1550nm	1550nm	1550nm
Aperture diameter $D$	5cm	8cm	5cm
Atmospheric structure constant $C_n^2$	$10^{-16} \text{ m}^{-2/3}$	$10^{-16} \text{ m}^{-2/3}$	$10^{-16} \text{ m}^{-2/3}$
Transmission distance $L$	14 km	14 km	30 km
Atmospheric coherent diameter $r_0$	25.6 cm	25.6 cm	16.2 cm
Log-amplitude standard deviation $\sigma$	0.25	0.25	0.5
Phase noise variance $\sigma_\phi^2$	0.07rad	0.15 rad	0.15 rad

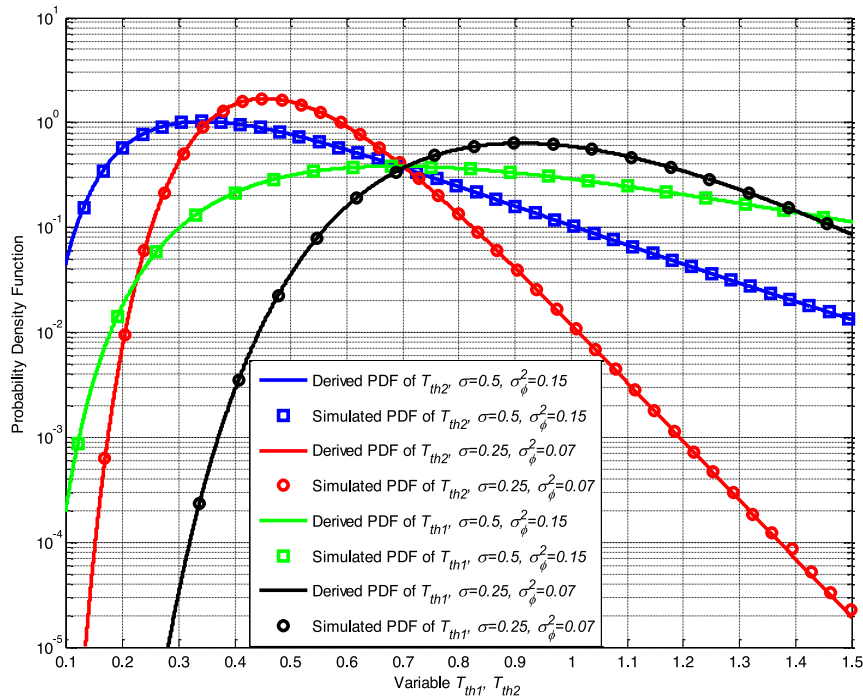


Fig. 4. The derived and simulated PDFs for  $T_{th1}$ ,  $T_{th2}$  of the CD-DADT system with double rapid detection thresholds over a lognormal fading channel.

where  $D$  is the aperture diameter,  $r_0$  is the Fried parameter and  $C_J = 1.0299$  [20]. For plane waves and Kolmogorov turbulence,  $r_0$  can be expressed as  $r_0 = 1.68(C_n^2 L k^2)^{-3/5}$  [21]. So, the optical turbulence parameters for our study can be set as Table 1.

Finally, we set the symbol rate of the system as 2Gbps and the length  $N$  of a frame with forward error correction (FEC) code as  $10^6$  bits during the simulation. The noise bandwidth is also assumed to be equal to the data rate in the rest of the paper.

As can be seen from Fig. 4, the analytical PDFs of the double rapid detection thresholds  $T_{th1}$  and  $T_{th2}$  are compared with the simulated PDFs of the double detection thresholds. Here, we set the optical turbulence parameters as Value I and Value III in Table 1. Monte Carlo computer simulations with  $10^8$  trials are used to obtain the simulated PDFs. The analytical PDF shows excellent agreement with the simulated PDF.

The following simulated BERs results are also obtained by the Monte Carlo computer simulations. The simulation process is given as follow. For the limitation of the computer's RAM (Random Access Memory), at first,  $10^6$  frames of random binary numbers with a length of  $1.5 \times 10^6$  are created and

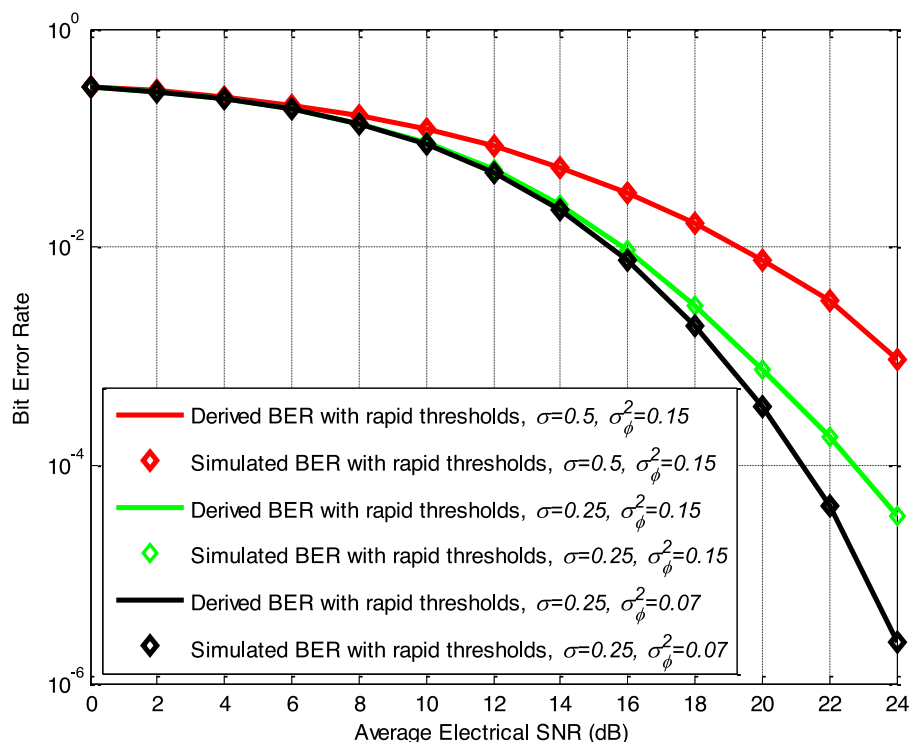


Fig. 5. The derived and simulated BERs of the CD-DADT systems using double rapid detection thresholds over lognormal turbulence channel.

stored in a file on the local hard disk. Then the binary sequences are read from the file and sent by different systems with different turbulences given in the Table 1. Finally, the simulated BERs can be achieved by comparing the final output binary sequences in the receivers with the frames in the file.

In Fig. 5, the derived and simulated BERs of the system using double rapid detection thresholds with different optical turbulence versus average electrical SNR at the receiver are plotted. The derived BERs show excellent agreement with the simulated BERs. Note that the rise of log-amplitude standard deviation and the phase noise variance leads to significant degradation in the error performance of the system. Combined with the Table 1, it shows that both transmission distance and aperture diameter will influence the system performance.

As can be seen from Fig. 6, the performances of the CD-DADT systems with different second threshold are evaluated for lognormal fading. Compared with the system with rapid detection threshold, the system with decision-aided threshold has better BER performance and there is an improvement of approximately 3 dB in SNR at the BER of  $10^{-3}$  when the optical turbulence parameters are set as Value I in Table 1.

The BERs versus received optical power for different systems are shown in Fig. 7, where the LO power of the CD-DADT systems is 5 dBm and the optical turbulence parameters is set as Value I in Table 1. The BER of  $10^{-3}$  is set as the benchmark, since under this BER error free transmission could be achieved by applying FEC code [14]. From Fig. 7, it can be seen that the CD-DADT system has higher sensitivity than other systems. For the system with fixed threshold detection and the source information transformation system, the required received optical powers to achieve BER of  $10^{-3}$  are  $-5.7$  dBm and  $-28.3$  dBm, respectively. For the CD-DADT systems with rapid detection threshold and decision-aided threshold, the required received optical powers for achieving the same BER are  $-32.8$  dBm and  $-35.8$  dBm, respectively. Hence, the power reduction by CD-DADT system using decision-aided threshold as the second threshold are 30.1 dB and 7.5 dB compared with the fixed threshold detection system and the source information transformation system.

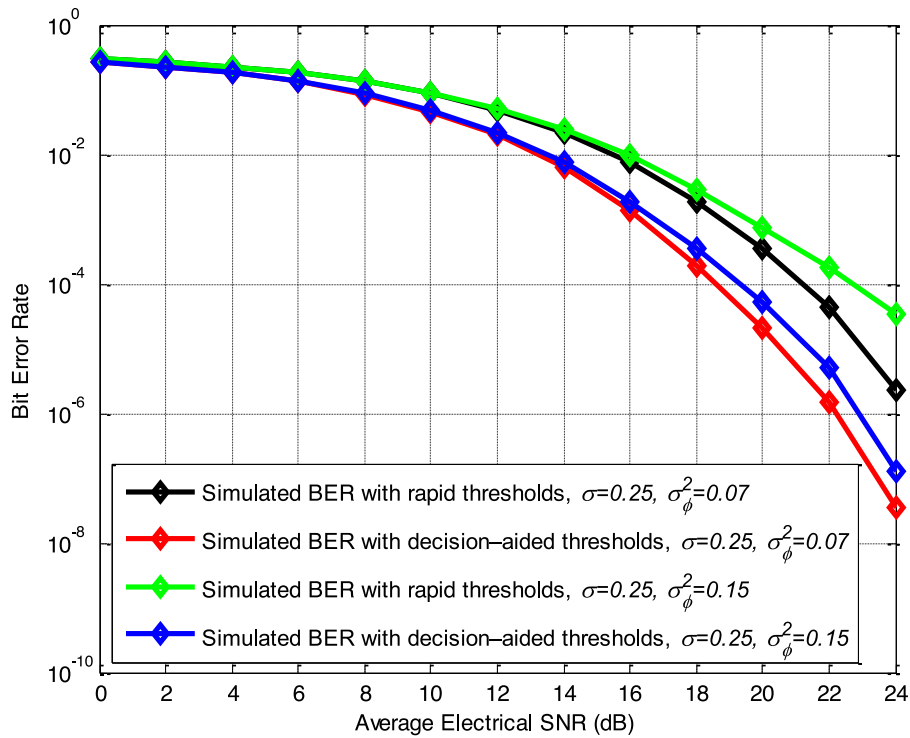


Fig. 6. The simulated BERs of the CD-DADT systems using rapid detection threshold and decision-aided threshold as the second threshold over lognormal turbulence channel.

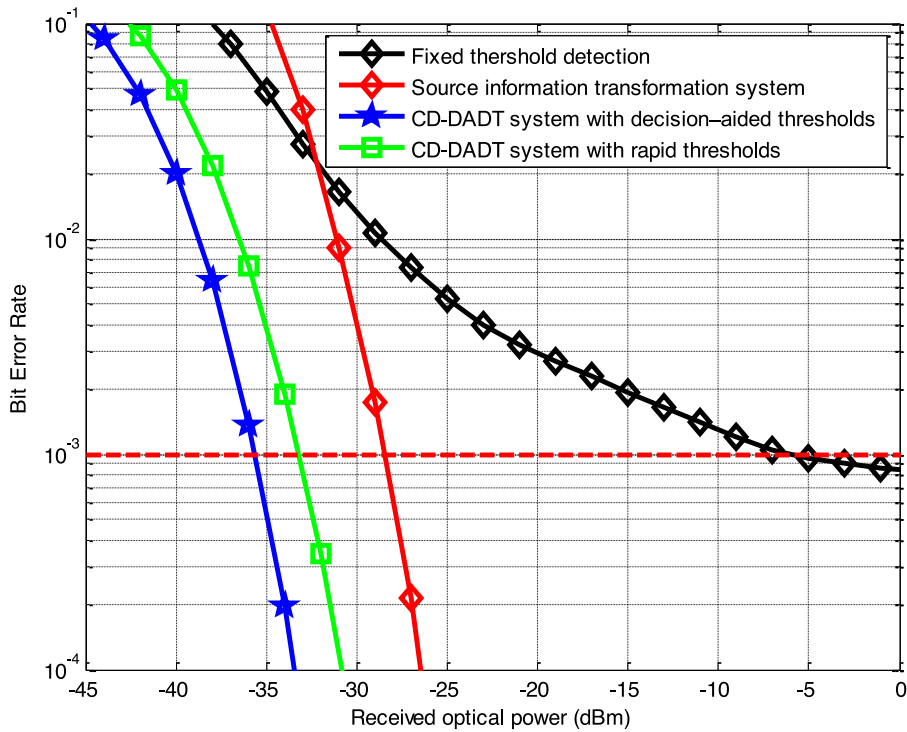


Fig. 7. BERs of different systems over lognormal turbulence channel with  $\sigma = 0.25$ ,  $\sigma_{\phi^2} = 0.07$ , LO power = 5 dBm.

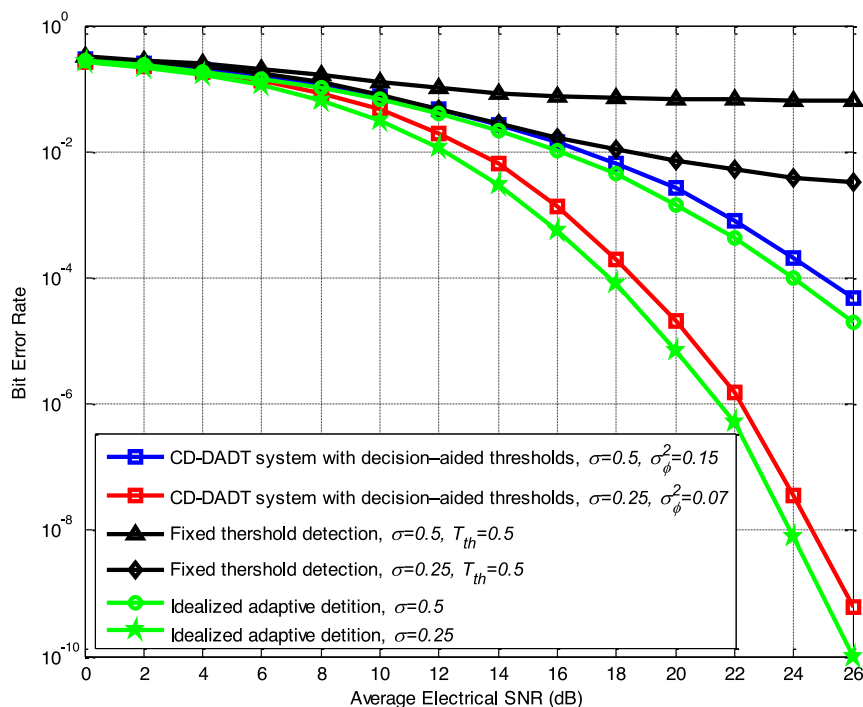


Fig. 8. The simulated BERs of the systems using idealized adaptive detection threshold, CD-DADT with decision-aided threshold, and fixed detection threshold over lognormal turbulence channel.

In Fig. 8, the average BER for the OOK system with a fixed detection threshold  $T_{th} = 0.5$ , the OOK system with idealized adaptive detection threshold, and the CD-DADT system with decision-aided threshold over lognormal fading channel under different turbulence conditions are plotted. Compared with the OOK IM/DD system with a fixed detection, the CD-DADT system with decision-aided threshold has better BER performance and can eliminate the error floor that appears in the large SNR regime. It is also seen in Fig. 8 that the OOK system with idealized adaptive detection threshold ( $T_{th} = h/2$ ) over a lognormal turbulence model with  $\sigma = 0.25$  requires a SNR of 24.8 dB to attain a BER of  $1 \times 10^{-9}$ , while the proposed system with  $\sigma = 0.25$  and  $\sigma_{\phi}^2 = 0.07$  requires a SNR of 25.8 dB to achieve the same BER performance. Thus, compared with the system with idealized adaptive detection thresholds, there is only 1 dB SNR penalty for the system using CD-DADT.

From Fig. 7 and Fig. 8, it is also can be seen that the BER of the system with fixed threshold seems to saturate for large SNR values, while in the low SNR regime the BER performance of the system with fixed threshold is almost the same as the BER performance of the CD-DADT system and the idealized adaptive detection threshold system. This is because the BERs of the systems in the low SNR regime are mainly affected by noise, while in high SNR regime the BERs are mainly affected by the atmospheric turbulence induced fading. Compared with the CD-DADT system and the idealized adaptive detection threshold system, the system with fixed threshold cannot adjust the thresholds according to the atmospheric turbulence induced fading. This leads to the phenomenon that the BER of the system with fixed threshold becomes saturated in the high SNR regime. However, in the low SNR regime, the CD-DADT system and the idealized adaptive detection threshold system focus more on the atmospheric turbulence induced fading than the noise, so the adaptive thresholds of other system cannot bring more BER gain than the fixed threshold to the systems because of the great influence of noise.

As can be seen from Fig. 9, the simulated BERs of the CD-DADT systems using decision-aided threshold and the system using source information transformation versus average electrical SNR are plotted. We set the normalized standard deviation of irradiance  $\sigma = 0.25$ . It is shown

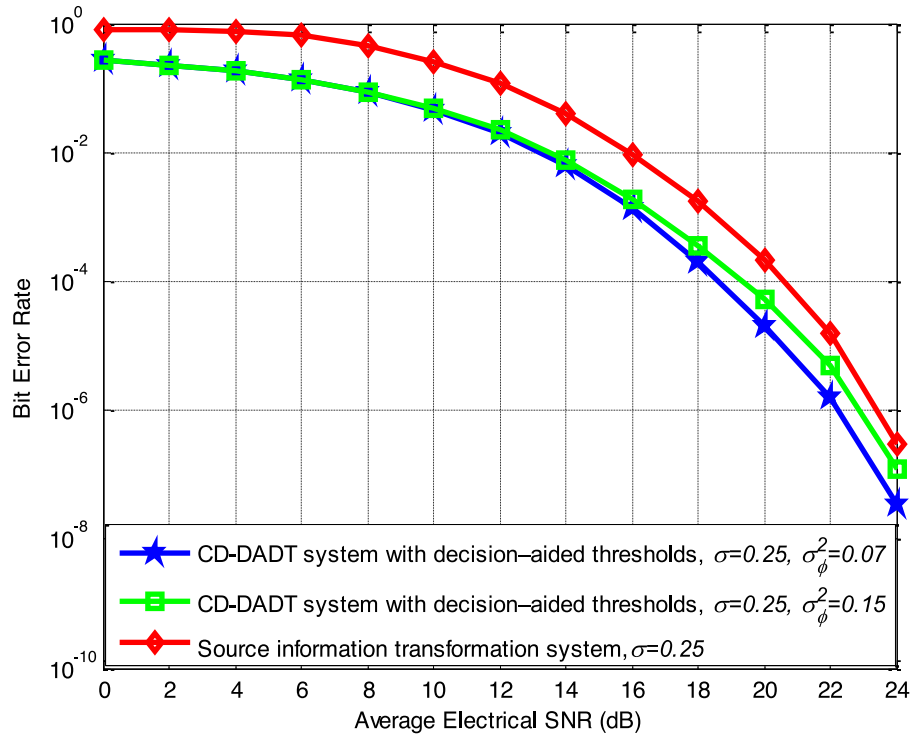


Fig. 9. The simulated BERs of the systems using CD-DADT with decision-aided threshold, source information transformation over lognormal turbulence channel.

that the BER performance of the CD-DADT system is better than that of the system using source information transformation. This is due to the fact that the system can eliminate the situation that binary sequence “00” is detected at the receiver with double adaptive detection thresholds (There is always a larger branch at the receiver which can be considered as “1”.) and offer better detection thresholds.

Therefore, as we can see in this section, the performance of the system is satisfactory and the analytical results show excellent agreement with the simulated results.

## 6. Conclusions

In this paper, the free-space optical communication systems using CD-DADT have been proposed. It is shown that the systems can achieve good BER performance with a low level of implementation complexity. The PDFs of the double rapid detection thresholds and average BER of the system have been also given in this paper. Simulated results show excellent agreement with the analytical results. Hence, the CD-DADT scheme can contribute to the performance improvement of the FSO system and its practical realization.

## Appendix

When the system transmits ternary symbol  $b_j$ , other conditional probabilities  $P(\hat{b}_j|b_j)$  of received ternary symbol  $\hat{b}_j$  can be written as follow:

$$P(1|0) = E_h \left[ E_{\varphi_n} \left[ P \left( h \sin(\varphi_n) + n_1 > h \cos(\varphi_n) + n_2 \cap \frac{h \sin(\varphi_n) + n_1}{2} > h \cos(\varphi_n) + n_2 \mid h, \varphi_n \right) \right] \right], \quad (38)$$

$$P(2|0) = E_h \left[ E_{\varphi_n} \left[ P \left( h \sin(\varphi_n) + n_1 > h \cos(\varphi_n) + n_2 \cap \frac{h \sin(\varphi_n) + n_1}{2} < h \cos(\varphi_n) + n_2 | h, \varphi_n \right) \right] \right] \\ + E_h \left[ E_{\varphi_n} \left[ P \left( h \cos(\varphi_n) + n_2 > h \sin(\varphi_n) + n_1 \cap \frac{h \cos(\varphi_n) + n_2}{2} < h \sin(\varphi_n) + n_1 | h, \varphi_n \right) \right] \right], \quad (39)$$

$$P(0|1) = E_h \left[ E_{\varphi_n} \left[ P \left( h \sin(\varphi_n) + n_2 > h \cos(\varphi_n) + n_1 \cap \frac{h \sin(\varphi_n) + n_2}{2} > h \cos(\varphi_n) + n_1 | h, \varphi_n \right) \right] \right], \quad (40)$$

$$P(1|1) = E_h \left[ E_{\varphi_n} \left[ P \left( h \cos(\varphi_n) + n_1 > h \sin(\varphi_n) + n_2 \cap \frac{h \cos(\varphi_n) + n_1}{2} > h \sin(\varphi_n) + n_2 | h, \varphi_n \right) \right] \right], \quad (41)$$

$$P(2|1) = E_h \left[ E_{\varphi_n} \left[ P \left( h \sin(\varphi_n) + n_2 > h \cos(\varphi_n) + n_1 \cap \frac{h \sin(\varphi_n) + n_2}{2} < h \cos(\varphi_n) + n_1 | h, \varphi_n \right) \right] \right] \\ + E_h \left[ E_{\varphi_n} \left[ P \left( h \cos(\varphi_n) + n_1 > h \sin(\varphi_n) + n_2 \cap \frac{h \cos(\varphi_n) + n_1}{2} < h \sin(\varphi_n) + n_2 | h, \varphi_n \right) \right] \right], \quad (42)$$

$$P(0|2) = E_h \left[ E_{\varphi_n} \left[ P \left( n_2 > n_1 \cap \frac{\sqrt{2}h \cos(\varphi_n - \frac{\pi}{4}) + n_2}{2} > \sqrt{2}h \cos(\varphi_n - \frac{\pi}{4}) + n_1 | h, \varphi_n \right) \right] \right], \quad (43)$$

$$P(1|2) = E_h \left[ E_{\varphi_n} \left[ P \left( n_1 > n_2 \cap \frac{\sqrt{2}h \cos(\varphi_n - \frac{\pi}{4}) + n_1}{2} > \sqrt{2}h \cos(\varphi_n - \frac{\pi}{4}) + n_2 | h, \varphi_n \right) \right] \right], \quad (44)$$

$$P(2|2) = E_h \left[ E_{\varphi_n} \left[ P \left( n_2 > n_1 \cap \frac{\sqrt{2}h \cos(\varphi_n - \frac{\pi}{4}) + n_2}{2} < \sqrt{2}h \cos(\varphi_n - \frac{\pi}{4}) + n_1 | h, \varphi_n \right) \right] \right] \\ + E_h \left[ E_{\varphi_n} \left[ P \left( n_1 > n_2 \cap \frac{\sqrt{2}h \cos(\varphi_n - \frac{\pi}{4}) + n_1}{2} < \sqrt{2}h \cos(\varphi_n - \frac{\pi}{4}) + n_2 | h, \varphi_n \right) \right] \right]. \quad (45)$$

## Acknowledgment

The authors would like to thank the Optical Communication Laboratory of CIOMP for the use of their equipment and they also thank the anonymous reviewers for their valuable suggestions.

## References

- [1] Z. Huang *et al.*, "Hybrid optical wireless network for future SAGO-integrated communication based on FSO/VLC heterogeneous interconnection," *IEEE Photon. J.*, vol. 9, no. 2, Apr. 2017, Art. no. 7902410.
- [2] Z. Wang, W. Zhong, S. Fu, and C. Lin, "Performance comparison of different modulation formats over free-space optical (FSO) turbulence links with space diversity reception technique," *IEEE Photon. J.*, vol. 1, no. 6, pp. 277–285, Dec. 2009.
- [3] K. L. Sterckx, J. M. H. Elmirghani, and R. A. Cryan, "On the use of adaptive threshold detection in optical wireless communication systems," *Proc. IEEE Conf. Global Telecommun.*, 2000, pp. 1242–1246.
- [4] L. Yang, J. Cheng, and J. F. Holzman, "Electrical-SNR-optimized detection threshold for OOK IM/DD optical wireless communications," in *Proc. 13th Can. Workshop Inf. Theory*, 2013, pp. 186–189.
- [5] L. Fei and L. Houbing, "Optimum detection threshold for free-space optical communication with atmospheric scintillation," in *Proc. Int. Conf. Optoelectron. Microelectron.*, 2015, pp. 191–196.
- [6] M. K. Simon and V. A. Vilnrotter, "Alamouti-type space-time coding for free-space optical communication with direct detection," *IEEE Trans. Wireless Commun.*, vol. 4, no. 1, pp. 35–39, Jan. 2005.
- [7] S. M. Haas and J. H. Shapiro, "Capacity of wireless optical communications," *IEEE J. Sel. Areas Commun.*, vol. 21, no. 8, pp. 1346–1357, Oct. 2003.

- [8] K. Chakraborty, "Capacity of the MIMO optical fading channel," in *Proc. Int. Symp. Inf. Theory*, 2015, pp. 530–534.
- [9] M. Jazayerifar and J. A. Salehi, "Atmospheric optical CDMA communication systems via optical orthogonal codes," *IEEE Trans. Commun.*, vol. 54, no. 9, pp. 1614–1623, Sep. 2006.
- [10] M. Uysal, J. Li, and M. Yu, "Error rate performance analysis of coded free-space optical links over gamma-gamma atmospheric turbulence channels," *IEEE Trans. Wireless Commun.*, vol. 5, no. 6, pp. 1229–1233, Jun. 2006.
- [11] X. Zhu and J. M. Kahn, "Pilot-symbol assisted modulation for correlated turbulent free-space optical channels," *Proc. SPIE*, vol. 4489, pp. 4498–4504, 2001.
- [12] H. Moradi, H. H. Refai, and P. G. LoPresti, "Thresholding-based optimal detection of wireless optical signals," *J. Opt. Commun. Netw.*, vol. 1, no. 5, pp. 452–462, 2009.
- [13] J. Li, J. Q. Liu, and D. P. Taylor, "Optical communication using subcarrier PSK intensity modulation through atmospheric turbulence channels," *IEEE Trans. Commun.*, vol. 55, no. 8, pp. 1598–1606, Aug. 2007.
- [14] Z. Wang, W. Zhong, and C. Yu, "Performance improvement of OOK free-space optical communication systems by coherent detection and dynamic decision threshold in atmospheric turbulence conditions," *IEEE Photon. Technol. Lett.*, vol. 24, no. 22, pp. 2035–2037, Nov. 2012.
- [15] L. Yang, B. Zhu, J. Cheng, and J. F. Holzman, "Free-space optical communications using ON–OFF keying and source information transformation," *J. Lightw. Technol.*, vol. 24, no. 12, pp. 4750–4762, Jun. 2006.
- [16] M. Khalighi, F. Xu, Y. Jaafar, and S. Bourennane, "Double-laser differential signaling for reducing the effect of background radiation in freespace optical systems," *J. Opt. Commun. Netw.*, vol. 3, no. 2, pp. 145–154, 2011.
- [17] X. Li *et al.*, "Performance improvement of coherent free-space optical communication with quadrature phase-shift keying modulation using digital phase estimation," *Appl. Opt.*, vol. 56, no. 16, pp. 4695–4701, 2017.
- [18] A. Jurado-Navas, J. M. Garrido-Balsells, M. Castillo-Vázquez, and A. Puerta-Notario, "An efficient rate-adaptive transmission technique using shortened pulses for atmospheric optical communications," *Opt. Exp.*, vol. 18, no. 16, pp. 17346–17363, 2010.
- [19] L. C. Andrews and R. L. Phillips, *Laser Beam Propagation Through Random Media*, 2nd ed. Bellingham, WA, USA: SPIE, 2005.
- [20] A. Belmonte and J. M. Khan, "Capacity of coherent free-space optical links using diversity-combining techniques," *Opt. Exp.*, vol. 17, no. 4, pp. 12601–12611, 2009.
- [21] D. L. Fried, "Optical heterodyne detection of an atmospherically distorted signal wave front," *Proc. IEEE*, vol. 55, no. 1, pp. 57–77, Jan. 1967.